Modular Kinetic Analysis of the Adenine Nucleotide Translocator–Mediated Effects of Palmitoyl-CoA on the Oxidative Phosphorylation in Isolated Rat Liver Mitochondria

Jolita Ciapaite,[1] Gerco Van Eikenhorst,[1] Stephan J.L. Bakker,[2] Michaela Diamant,[3] Robert J. Heine,[3] Marijke J. Wagner,[1] Hans V. Westerhoff,[1] and Klaas Krab[1]

To test whether long-chain fatty acyl-CoA esters link obesity with type 2 diabetes through inhibition of the mitochondrial adenine nucleotide translocator, we applied a system-biology approach, dual modular kinetic analysis, with mitochondrial membrane potential (Δψ) and the fraction of matrix ATP as intermediates. We found that 5 μmol/l palmitoyl-CoA inhibited adenine nucleotide translocator, without direct effect on other components of oxidative phosphorylation. Indirect effects depended on how oxidative phosphorylation was regulated. When the electron donor and phosphate acceptor were in excess, and the mitochondrial "work" flux was allowed to vary, palmitoyl-CoA decreased phosphorylation flux by 38% and the fraction of ATP in the medium by 39%. Δψ increased by 15 mV, and the fraction of matrix ATP increased by 46%. Palmitoyl-CoA had a stronger effect when the flux through the mitochondrial electron transfer chain was maintained constant: Δψ increased by 27 mV, and the fraction of matrix ATP increased 2.6 times. When oxidative phosphorylation flux was kept constant by adjusting the rate using hexokinase, Δψ and the fraction of ATP were not affected. Palmitoyl-CoA increased the extramitochondrial AMP concentration significantly. The effects of palmitoyl-CoA in our model system support the proposed mechanism linking obesity and type 2 diabetes through an effect on adenine nucleotide translocator. *Diabetes* 54:944–951, 2005

Obesity is a common finding in patients with type 2 diabetes (1–3). Numerous studies suggest that the oversupply of lipid to nonadipose tissues might result in lipotoxicity and contribute to the development of the insulin resistance syndrome and type 2 diabetes (4,5). The molecular mechanisms responsible for lipotoxicity, insulin resistance, and β-cell dysfunction are not fully understood. It is particularly confusing that so many processes appear to be affected at the same time, but not always to the same extent, and often in paradoxical ways.

It has been hypothesized that inhibition of the mitochondrial adenine nucleotide translocator by long-chain fatty acyl-CoA esters, the active form of fatty acids, may be an important link between obesity and type 2 diabetes (6,7). Adenine nucleotide translocator is an enzyme that catalyzes the exchange of mitochondrial ATP for cytosolic ADP (8). It was shown that long-chain fatty acyl-CoA esters are potent inhibitors of adenine nucleotide translocator from both the cytosolic and the matrix side of the inner mitochondrial membrane (9). It was proposed that accumulation of long-chain fatty acyl-CoA esters in the cell and subsequent inhibition of adenine nucleotide translocator could lead to an increase in the matrix ATP-to-ADP ratio, membrane potential (Δψ; i.e., electric potential across the inner mitochondrial membrane [out minus in]), and oxygen free radical production. In β-cells, like in other cells (10), an initial increase in $O_2^{\bullet-}$ (superoxide anion radical) production could stimulate cell growth and contribute to compensatory hyperinsulinemia. Later on, sustained high levels of $O_2^{\bullet-}$ should result in a decline in β-cell function and viability. Moreover, the inhibition of adenine nucleotide translocator was proposed to decrease the cytosolic ATP-to-ADP ratio and shift the equilibrium of the adenylate kinase toward production of ATP and AMP. The increase in AMP concentration should promote formation of adenosine, which in turn was reported to have both inhibitory and stimulatory effects on insulin-dependent glucose uptake (11–13). It was hypothesized that an increased extracellular adenosine concentration could explain such pathophysiological features of type 2 diabetes as elevated levels of uric acid, increased sympathetic activity, and expansion of extracellular volume (9). For

From the [1]Department of Molecular Cell Physiology, Institute for Molecular Cell Biology, BioCenter Amsterdam, Faculty of Earth and Life Sciences, Vrije Universiteit, Amsterdam, the Netherlands; the [2]Department of Internal Medicine, University Hospital Groningen, Groningen, the Netherlands; and the [3]Department of Endocrinology, Institute for Cardiovascular Research, Vrije Universiteit Medical Center, Amsterdam, the Netherlands.

Address correspondence and reprint requests to Klaas Krab, Department of Molecular Cell Physiology, Institute for Molecular Cell Biology, BioCenter Amsterdam, Faculty of Earth and Life Sciences, Vrije Universiteit, De Boelelaan 1085, NL-1081 HV Amsterdam, the Netherlands. E-mail: klaas@bio.vu.nl.

Received for publication 6 July 2004 and accepted in revised form 4 January 2005.

Ap5A, P^1P^5-di(adenosine-5′) pentaphosphate; TPP^+, tetraphenylphosphonium ion.

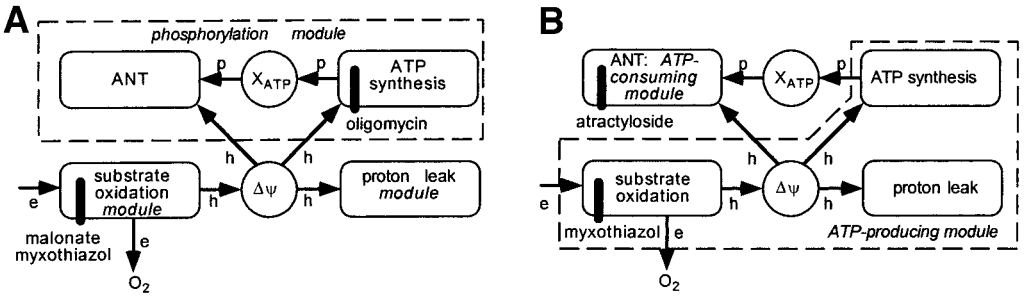

FIG. 1. Division of oxidative phosphorylation into modules. Arrows marked "e," "h," and "p" indicate electron flux, transmembrane proton flux, and ATP flux, respectively. The sites of action of the inhibitors used are indicated. *A*: Membrane potential (Δψ) as connecting intermediate. *B*: Fraction of matrix ATP (X_{ATP}) as intermediate. ANT, adenine nucleotide translocator.

this reason, quantification of adenine nucleotide translocator inhibition by long-chain fatty acyl-CoA esters is important to test its putative key role in the development of type 2 diabetes and associated complications.

A powerful method to quantify the effects of substances on complex systems is provided by modular kinetic analysis (rev. in 14). Figure 1*A* shows how the system of interest (mitochondrial oxidative phosphorylation) is divided into three functional modules, interacting with the linking intermediate membrane potential (Δψ). To obtain a kinetic characterization of, for example, the phosphorylation module, the steady-state values of the flux through this module and the value of Δψ are measured, whereas another module (e.g., the substrate oxidation module) is titrated with an inhibitor of that module (e.g., myxothiazol). A plot of the phosphorylation flux against Δψ then serves as a kinetic characterization of the phosphorylation module. To determine the effect of long-chain fatty acyl-CoA esters on the phosphorylation module, the procedure is repeated in the presence of these esters. Interaction of long-chain fatty acyl-CoA esters with the phosphorylation module is then detected as a change in the plot of the phosphorylation flux against Δψ. Figure 1*B* shows a different division into two modules, with the fraction of matrix ATP as linking intermediate. A combination of these leads to precise determinations of which parts of the system are affected by long-chain fatty acyl-CoA esters and which are not.

In this study we tested part of the hypothesis that considers the effect of long-chain fatty acyl-CoA esters on adenine nucleotide translocator, Δψ, and both intra- and extramitochondrial ATP-to-ADP ratio in a model system consisting of isolated rat liver mitochondria. We tested the effect of palmitoyl-CoA, a derivative of palmitic acid, one of the most abundant long-chain fatty acids (15). To measure the fraction of matrix ATP, we used a novel indirect method in which extraction of total adenine nucleotides is combined with determination of the extramitochondrial fraction of ATP via the kinetics of hexokinase. We found that the results supported the hypothesis.

RESEARCH DESIGN AND METHODS

Hexokinase, glucose-6-phosphate dehydrogenase, pyruvate kinase + lactate dehydrogenase, and creatine kinase were purchased from Roche (Mannheim, Germany). Oligomycin, myxothiazol, atractyloside, palmitoyl-CoA, pyruvate kinase, myokinase, P^1P^5-di(adenosine-5′) pentaphosphate (Ap5A), and Fluka AR20 and AR1000 silicone oil were obtained from Sigma Aldrich.

Isolation of mitochondria. Liver mitochondria were isolated from male Wistar rats (250–300 g) as previously described (16), using 250 mmol/l sucrose, 10 mmol/l Tris-HCl, 3 mmol/l EGTA, and 2 mg/ml BSA, pH 7.7, as the isolation medium. Protein content was determined according to Bradford (17), with BSA as the standard.

Oxygen uptake and membrane potential measurements. Mitochondria were incubated at 25°C in a closed, stirred, and thermostatted glass vessel equipped with a Clark-type oxygen electrode and a tetraphenylphosphonium ion (TPP^+)-sensitive electrode (A. Zimkus, Vilnius State University, Vilnius, Lithuania), allowing simultaneous monitoring of Δψ and oxygen uptake. For each incubation the TPP^+-sensitive electrode was calibrated with TPP bromide to a final concentration of 400 nmol/l. Δψ was calculated from the distribution of TPP^+ using a TPP^+ binding correction factor of 0.16 μl/mg protein (18,19).

The reaction medium contained 25 mmol/l creatine and 25 mmol/l creatine phosphate (both present to allow determination of hexokinase kinetics in the identical medium, see below), 75 mmol/l KCl, 20 mmol/l Tris, 2.3 mmol/l $MgCl_2$, 10 mmol/l succinate, 2.0 μmol/l rotenone, and 50 μmol/l Ap5A, pH 7.3. Palmitoyl-CoA was added from a 2-mmol/l stock solution in water. An ADP-regenerating system consisting of excess hexokinase (5.78 units/ml), glucose (12.5 mmol/l), and phosphate (5.0 mmol/l KH_2PO_4) was used to maintain steady-state respiration rates. Finally, 100 μmol/l ATP was added to initiate state 3 respiration.

Determination of the adenine nucleotide concentrations. Adenine nucleotides were extracted with hot phenol as previously described (20). The ATP concentration was measured in the water phase, using a luciferin-luciferase ATP monitoring kit (Bio-Orbit, Turku, Finland), following the recommendations of the manufacturer. ADP concentration was determined in the same sample after the addition of phosphoenolpyruvate (2.0 mmol/l) and pyruvate kinase (0.45 units/ml). AMP concentration was determined spectrophotometrically using a standard enzymatic assay (21).

Measurement of the phosphorylation rate. The rate of oxidative phosphorylation was measured as the rate of glucose-6-phosphate formation by hexokinase, as previously described (22). Glucose-6-phosphate was extracted with perchloric acid (0.7 mol/l), and samples were neutralized with a predetermined volume of 2 mol/l KOH/0.3 mol/l MOPS to a final pH of 7.0–7.2. The glucose-6-phosphate concentration in the extracts was determined spectrophotometrically using a standard enzymatic assay (23).

Measurement of the ADP-to-O ratio. The number of ADP molecules phosphorylated per oxygen atom reduced (ADP-to-O ratio) was determined in the same medium as the oxygen uptake and Δψ measurements, as previously described (24). The medium containing 1 mg of mitochondrial protein/ml was supplemented with 10 mmol/l succinate, 2 μmol/l rotenone, and 50 μmol/l Ap5A (to inhibit mitochondrial adenylate kinase). Then, 400 μmol/l ADP was added, and the increase in oxygen uptake rate was recorded. The amount of oxygen taken up during state 3 was corrected for proton leak–driven respiration at the same value of Δψ as described elsewhere (25). The ADP-to-O ratio was calculated by dividing the exact amount of added ADP by this corrected oxygen consumption.

Determination of ATP concentration in the mitochondrial matrix. To distinguish between the medium (100 μmol/l) and the matrix (circa 10 μmol/l) adenine nucleotide pools, we developed a new method in which ATP concentration in the medium is deduced from the flux through externally added hexokinase. The ATP concentration in the matrix is then calculated from the ATP in the reaction medium and the total ATP (matrix + reaction medium). Further in the text, we use fraction of ATP instead of ATP concentration. The fraction of ATP in the medium (r_{medium}) is defined as:

$$r_{medium} = \frac{[ATP_{medium}]}{[ATP_{medium}] + [ADP_{medium}]} \quad (1)$$

The fraction of matrix ATP is defined as:

$$r_{matrix} = \frac{[ATP_{matrix}]}{[ATP_{matrix}] + [ADP_{matrix}]} \quad (2)$$

Determination of the kinetics of hexokinase. The kinetics of hexokinase were determined in a system consisting of the coupled enzymes creatine kinase, hexokinase, and glucose-6-phosphate dehydrogenase (Fig. 2). The reaction rate of hexokinase was determined spectrophotometrically after the appearance of NADPH (in the absence of mitochondria), as previously

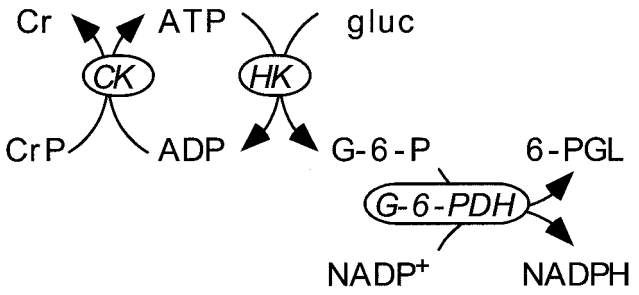

FIG. 2. Scheme of experimental setup for determination of hexokinase kinetics. Cr, creatine; CrP, creatine phosphate; CK, creatine kinase; HK, hexokinase; G-6-P, glucose-6-phosphate; G-6-PDH, glucose-6-phosphate dehydrogenase; gluc, glucose; 6-PGL, 6-phosphoglucolactone.

described (26). Different steady-state rates of the hexokinase reaction were obtained by varying the amount of creatine kinase. Hexokinase steady-state rate measurements were carried out at the same temperature and in the same reaction medium as mitochondrial respiration measurements, with 12.5 mmol/l glucose and 100 μmol/l ADP as substrates. For each steady state, a sample for determination of adenine nucleotide concentrations was taken. Figures 3*A* and *B* show these experimentally determined kinetics of hexokinase. The line fitted to the experimental points was used to deduce the fraction of ATP in the medium from the flux through hexokinase in the experiments with mitochondria.

Determination of the fraction of ATP in the medium. In the system with mitochondria, the flux through hexokinase is estimated from the oxygen uptake rate and ADP-to-O ratio. It was crucial that the total amount of nucleotides in this experiment be equal to the total amount of nucleotides in the reaction medium in the experiments with isolated enzymes. The experimentally determined ADP-to-O ratio was 1.89 ± 0.02 (n = 9). The addition of 5 μmol/l palmitoyl-CoA did not affect this ratio. In Fig. 3*C* the measured phosphorylation flux is plotted against that calculated from the oxygen uptake rate during titrations with malonate and myxothiazol. It is clear from these experiments that there are no significant variations of the ADP-to-O ratio during these inhibitor titrations.

Determination of the fraction of matrix ATP. After every measurement of the steady-state respiration rate of mitochondria, samples for extraction of total ATP and ADP (matrix + medium) were taken. The amount of ADP + ATP in the mitochondrial matrix was determined in a separate extraction in the absence of added adenine nucleotides. The phosphorylation flux was calculated from the oxygen uptake rate after the addition of ATP (corrected for leak-driven respiration at the same value of Δψ) and the ADP-to-O ratio. Then, the fraction of ATP in the medium was derived from this rate and the kinetic characteristics of the hexokinase. From these, the fraction of matrix ATP (r_{matrix}) was calculated as:

$$r_{matrix} = \frac{[ATP_{total}] - ([\{ATP_{total}\} + \{ADP_{total}\}] - [\{ATP_{matrix}\} + \{ADP_{matrix}\}]) \cdot r_{medium}}{[ATP_{matrix}] + [ADP_{matrix}]} \quad (3)$$

The limitation of our method is that it can only be used for relatively low total adenine nucleotide concentration without introducing significant error. Also, we have noted that even in the presence of the inhibitor of adenylate kinase, some AMP was formed (7.8 ± 0.3 μmol/l, n = 2), decreasing the sum of medium ADP + ATP. We have checked that this decrease did not significantly affect the determination of the nucleotide concentrations in the matrix. Figure 3*B* shows that the kinetics of hexokinase in the part used for the determination of matrix ATP and ADP concentrations (0–400 nmol ADP/min) was similar when the total adenine nucleotide concentration decreased by 10–20 μmol/l. In the hexokinase titration experiments, adenine nucleotides in the matrix and in the medium were determined after separation of mitochondria from the medium by centrifuging 0.5 ml of the sample through 0.5 ml of the silicone oil (density 1.04 g/ml) layer into 0.5 ml of $HClO_4$ (0.7 mol/l), as previously described (27).

Data presentation. Data are the means ± SE. The listed n values represent the number of experiments performed on the independent mitochondrial preparations. Statistical differences were determined using the paired Student's t test. $P < 0.05$ was considered to be statistically significant.

RESULTS

Determining the site of action of palmitoyl-CoA. To determine the sites of the oxidative phosphorylation affected by palmitoyl-CoA, we applied the dual modular kinetic analysis described above. This method can be used because during measurements the system is in steady state, as judged from the time-independency of oxygen-uptake flux and Δψ (not shown). First, oxidative phosphorylation was conceptually divided into three modules connected by Δψ as the intermediate (Fig. 1*A*). Although the true connecting intermediate among the modules of the oxidative phosphorylation is $\Delta\mu_H^+$ (protonmotive force, i.e. the electrochemical potential difference for protons across the inner mitochondrial membrane [out minus in]) it was shown previously that in a reaction medium containing excess inorganic phosphate (P_i) (as in our experimental conditions), contribution of the pH difference across the mitochondrial membrane (ΔpH) to the value of $\Delta\mu_H^+$ is relatively small compared with that of Δψ and does not change significantly under different phosphorylating conditions (18,19,28,29). Therefore, Δψ can be

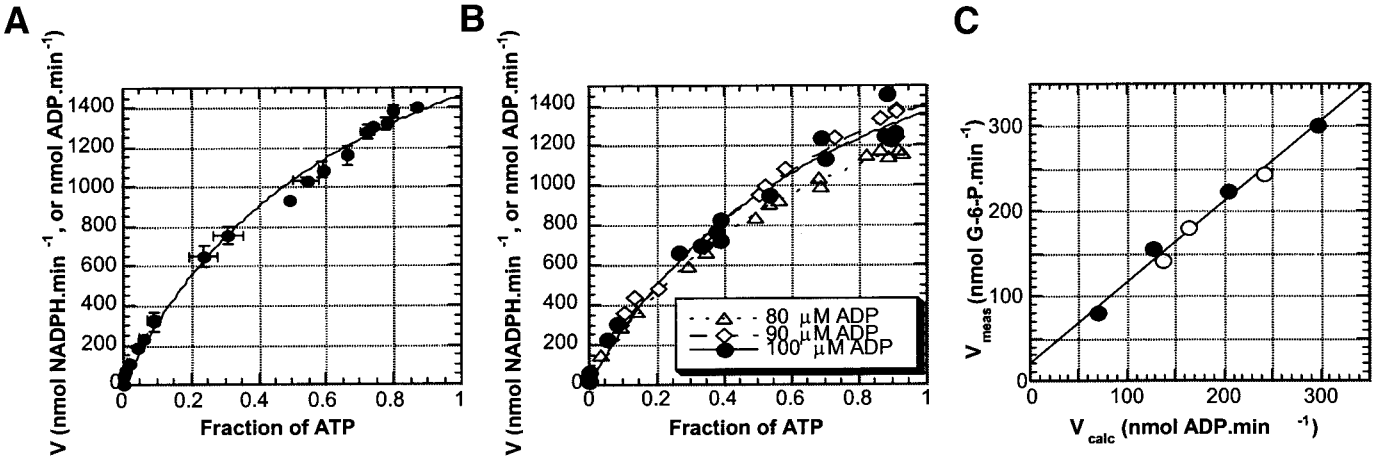

FIG. 3. Hexokinase kinetics. *A*: Hexokinase kinetics with 100 μmol/l ADP (n = 3). *B*: Hexokinase kinetics with different concentrations of added ADP. ●, 100 μmol/l ADP; ◇, 90 μmol/l ADP; △, 80 μmol/l ADP (n = 1). *C*: Comparison of calculated and measured phosphorylation flux (V) (n = 1). Measured flux is plotted against calculated flux. ●, rate titrated with malonate; ○, rate titrated with myxothiazole. Error bars: ± SE.

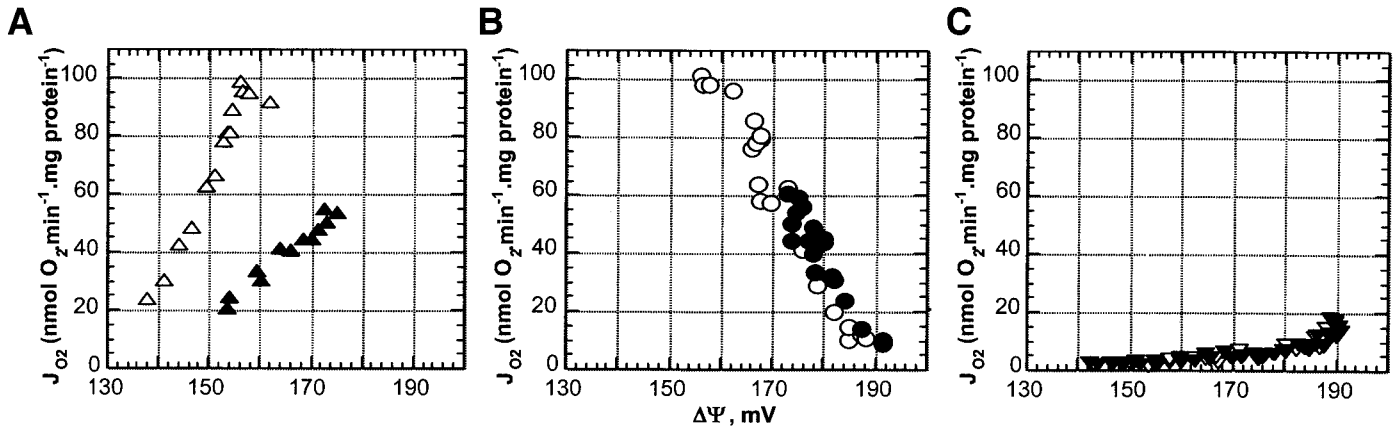

FIG. 4. Effect of palmitoyl-CoA on the kinetics of the modules of oxidative phosphorylation (connecting intermediate: Δψ). *A*: Kinetics of the phosphorylating module (oxygen uptake rate [J_{O2}] is corrected for proton leak rate at the same value of Δψ) determined by titration of the substrate oxidation module with 0–20 nmol/l myxothiazol. *B*: Kinetics of substrate oxidation module, determined by titration of the phosphorylating module with 0–0.3 μmol/l oligomycin. *C*: Kinetics of proton leak module, determined by titration of the substrate oxidation module with 0–1.25 mmol/l malonate in the presence of 0.3 μmol/l oligomycin. Open symbols: control; closed symbols: + 5 μmol/l palmitoyl-CoA.

used instead of $\Delta\mu_H^+$ as the connecting intermediate among the modules without introducing significant error. Starting from state 3 (regenerating ADP by excess hexokinase and glucose) with succinate as substrate, the responses of the kinetics of each of the modules to the addition of palmitoyl-CoA were determined by titration with an appropriate inhibitor. Figure 4 shows the effect of 5 μmol/l palmitoyl-CoA on the kinetic response of the three modules. We found that 5 μmol/l palmitoyl-CoA exclusively inhibited the phosphorylation reaction module (Fig. 4*A*). It had no significant effect on either the substrate oxidation module (Fig. 4*B*) or the proton leak (Fig. 4*C*).

In this approach adenine nucleotide translocator is part of the phosphorylating module. To determine the effect of palmitoyl-CoA explicitly on the adenine nucleotide translocator, we applied the modular kinetic analysis a second time. Oxidative phosphorylation was divided into two modules, with the fraction of matrix ATP as intermediate (Fig. 1*B*). Figure 5 shows the kinetic responses of these two modules. It is clear that 5 μmol/l palmitoyl-CoA inhibited the ATP-consuming module (Fig. 5*A*) and had hardly any effect on the ATP-producing module (including the respiratory chain and ATP synthase) (Fig. 5*B*). We conclude that the inhibition of the ATP-consuming module is caused by the inhibition of adenine nucleotide translocator because 5 μmol/l palmitoyl-CoA does not inhibit hexokinase under the experimental conditions used (results not shown).

Figures 4 and 5 together show that 5 μmol/l palmitoyl-CoA exclusively inhibits the adenine nucleotide translocator and has no direct effect on any other component of oxidative phosphorylation. Results shown in Fig. 6 support this conclusion because inhibition of phosphorylation with increasing concentrations of palmitoyl-CoA gave similar results as with atractyloside, a specific inhibitor of the adenine nucleotide translocator. Because the rate decreases with increasing palmitoyl-CoA concentration, and the palmitoyl-CoA points are on the atractyloside curve, we conclude that at a concentration between 0 and 20 μmol/l, palmitoyl-CoA indeed has an exclusive inhibitory effect on the adenine nucleotide translocator module.

The effects of palmitoyl-CoA on mitochondrial oxidative phosphorylation under different phosphorylating conditions. In vivo, both the redox potential input to the mitochondria and the availability of the substrate for the dephosphorylation of the ATP produced may vary depending on the state of the cell. Therefore, in addition to the situation where substrates for both respiration and phosphorylation are in excess, we considered two alternative situations that may also occur in vivo: *1*) constant limiting redox-equivalent supply-flux, referring to the physiological condition where mitochondrial function is

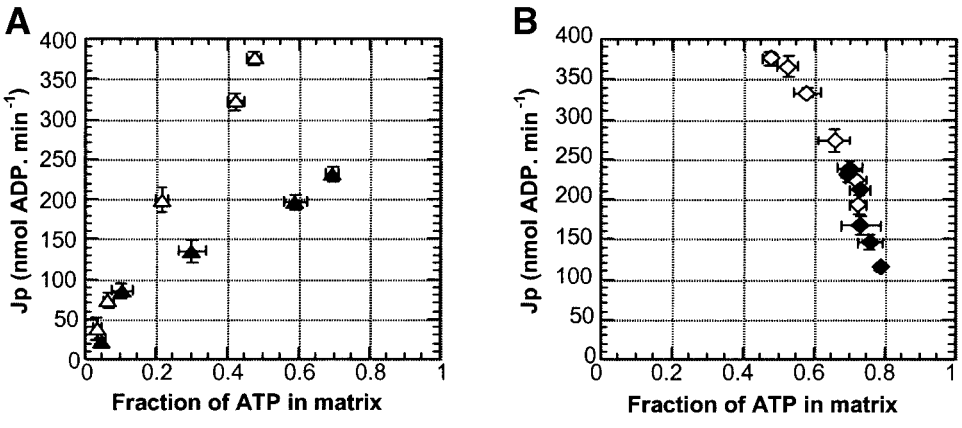

FIG. 5. Effect of palmitoyl-CoA on the kinetics of the modules of oxidative phosphorylation (connecting intermediate: fraction of matrix ATP). *A*: Kinetics of ATP-consuming module determined by titration of the ATP-producing module with 0–20 nmol/l myxothiazol (n = 10). *B*: Kinetics of ATP-producing module determined by titration of the ATP-consuming module with 0–1.5 μmol/l atractyloside (n = 4). Open symbols: control; closed symbols: + 5 μmol/l palmitoyl-CoA. Total concentration of matrix ATP + ADP = 11.4 ± 0.4 nmol/mg protein. Error bars: ± SE. Jp, phosphorylation flux.

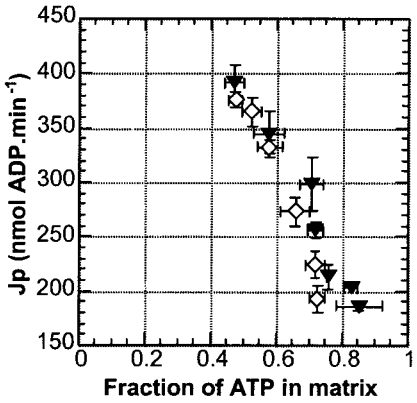

FIG. 6. Comparison of the effects of palmitoyl-CoA and atractyloside on phosphorylation flux and fraction of matrix ATP. Open symbols, titration with atractyloside (data from Fig. 5*B*, control); closed symbols, titration with 0–20 μmol/l palmitoyl-CoA ($n = 3$). Error bars: ± SE. Jp, phosphorylation flux.

set by the supply of redox equivalents, and *2*) a constant workload flux (i.e., when the extramitochondrial ATP utilization determines mitochondrial function).

The effects of palmitoyl-CoA on mitochondrial oxidative phosphorylation under three different conditions can be seen in Table 1. A comparison between *rows A* and *B* in Table 1 shows the effects of palmitoyl-CoA on oxidative phosphorylation under conditions of constant excess of ADP and glucose and ample redox equivalent supply. The addition of 5 μmol/l palmitoyl-CoA reduced the phosphorylation rate by 38% ($n = 16, P < 0.05$) and increased $\Delta\psi$ by 15 mV ($n = 4, P < 0.05$). Because $\Delta\psi$ was calculated from TPP^+ redistribution, the values we report are estimates only (30). The fraction of matrix ATP increased by 46% ($n = 16, P < 0.05$). The extramitochondrial fraction of ATP decreased by 39% ($n = 16, P < 0.05$).

The limited redox equivalent supply flux to the mitochondria can be mimicked by inhibiting electron flow in the mitochondrial respiratory chain with myxothiazol, inhibitor of complex III of the mitochondrial respiratory chain (Figs. 4*A* and 5*A*). In *row C* of Table 1, the situation is presented where the redox equivalent supply flux to the mitochondria is inhibited to a level similar to that obtained with 5 μmol/l palmitoyl-CoA added. At this virtually identical electron transfer rate, palmitoyl-CoA had a much stronger effect (*row B* minus *row C*) on both $\Delta\psi$ (it increased by 27 mV [$n = 10, P < 0.05$]) and the intramitochondrial fraction of ATP (it increased 2.6 times [$n = 10, P < 0.05$]).

The third condition we considered was that of a constant workload flux, established by the ATP-consuming branch (adenine nucleotide translocator + externally added hexokinase). Different extramitochondrial ATP utilization rates were achieved by adding different amounts of hexokinase. The dependence of the oxygen uptake rate on ATP concentrations in the mitochondrial matrix (Fig. 7*A*) and in the medium (Fig. 7*B*), as well as its dependence on the membrane potential (Fig. 7*C*), were measured. From this experiment the fraction of matrix ATP, the fraction of ATP in the medium, and the value of $\Delta\psi$ at the same phosphorylation flux as in the presence of 5 μmol/l palmitoyl-CoA were derived (Table 1, *row D*). In contrast to the previous conditions, the differences in $\Delta\psi$ and the intramitochondrial fractions of ATP (*row B* minus *row D*) were negligible. In this case the extramitochondrial fraction of ATP in the control was more than four times higher than in the presence of 5 μmol/l palmitoyl-CoA ($n = 3, P < 0.05$). From this we conclude that the effects of palmitoyl-CoA depend on the working conditions of the mitochondrial oxidative phosphorylation.

The effects of palmitoyl-CoA on the extramitochondrial AMP concentration. AMP is produced in the reaction ATP + AMP ↔ 2ADP catalyzed by adenylate kinase in the mitochondrial intermembrane space (31). When there is no inhibitor of adenylate kinase in the reaction medium, it is expected that the decrease in the external ATP-to-ADP ratio caused by palmitoyl-CoA will shift the adenylate kinase reaction toward the production of more ATP and buffer the change in the external ATP-to-ADP ratio. We have tested the effect of two concentrations of palmitoyl-CoA (5 and 10 μmol/l) on the concentration of the external (medium) AMP. The experimental conditions were as in the previous experiments with excess redox substrates and excess ADP, except that instead of 100 μmol/l, we used 2 mmol/l ATP (this higher ATP concentration, which is realistic physiologically, was chosen to obtain measurable AMP concentrations). The addition of palmitoyl-CoA to mitochondria respiring on succinate indeed led to an increase in AMP concentration from 77 ± 10 μmol/l in control to 88 ± 9 μmol/l ($n = 3, P < 0.05$) and 134 ± 6 μmol/l ($n = 3, P < 0.05$) for 5 and 10 μmol/l palmitoyl-CoA, respectively.

DISCUSSION

Long-chain fatty acyl-CoA esters are the key intermediates in lipid biosynthesis and degradation. There is much evidence that these esters have an important function in the regulation of cellular metabolism and gene expression (rev. in 32). Reported values of the total intracellular

TABLE 1
Effect of 5 μmol/l palmitoyl-CoA on oxidative phosphorylation under different conditions

	Fraction ATP in	Fraction ATP out	ΔΨ (mV)	J_{phos} (nmol ADP · min^{-1} · mg $prot^{-1}$)	J_O (nmol O_2 · min^{-1} · mg $prot^{-1}$)
A	0.48 ± 0.02	0.13 ± 0.005	158.6 ± 0.9	376 ± 7	102 ± 2
B	0.70 ± 0.02	0.08 ± 0.006	173.9 ± 0.4	232 ± 9	67 ± 3
C	0.27 ± 0.03	0.08 ± 0.003	147.2 ± 0.8	—	(set to 67)
D	0.73 ± 0.01	0.35 ± 0.035	172.8 ± 1.4	(set to 232)	—

Row A: Control at state 3 (excess substrate, excess ADP because of excess added hexokinase). Row B: State 3 with 5 μmol/l palmitoyl-CoA. Row C: Redox supply limited by 7.5 nmol/l myxothiazol, at the same value of the redox equivalent flux as row B. Row D: Constant work-load flux, at the same ATP consumption flux as row B (by lowering of hexokinase from 5.78 to 0.5 units/ml). $\Delta\psi$, mitochondrial membrane potential; J_O, oxidation rate; J_{phos}, phosphorylation rate; prot, protein.

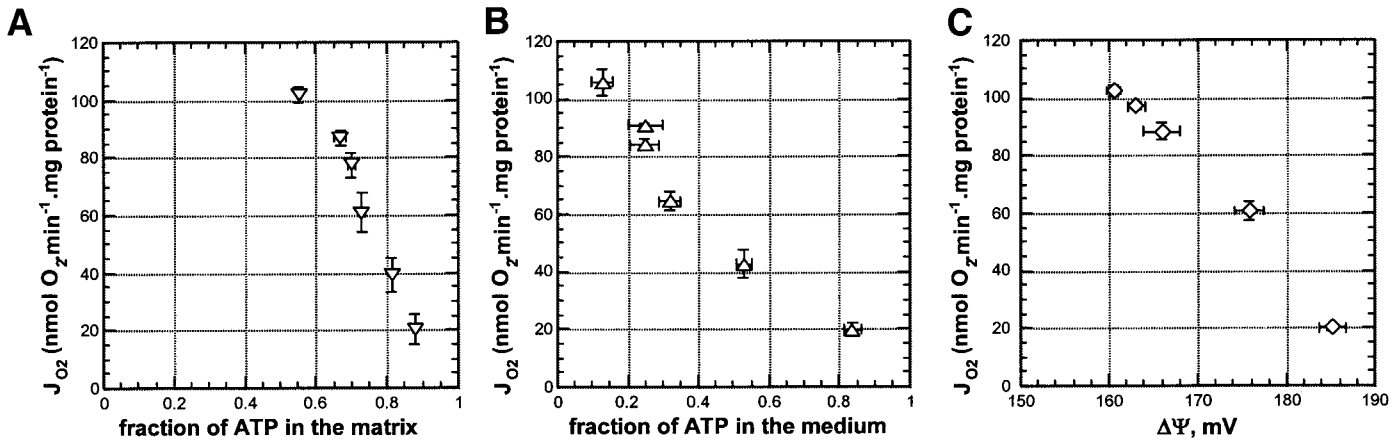

FIG. 7. Effect of hexokinase concentration on oxygen uptake rate (J_{O2}), matrix ATP concentration (*A*), medium ATP concentration (*B*), and Δψ (*C*) (n = 3). Adenine nucleotide concentration in the matrix and in the medium was determined after separation with silicone oil. Error bars: ± SE.

long-chain fatty acyl-CoA ester concentration vary from 5 to 160 μmol/l, depending on the tissue and the metabolic state of the cell (32). Concentrations of these esters increase significantly in the fasting state and under diabetic conditions (33,34). Despite these findings, there is an ongoing discussion as to whether this increase in the intracellular long-chain fatty acyl-CoA ester concentration has any consequences for cellular metabolism because the free concentration of cellular long-chain fatty acyl-CoA esters is expected to be tightly regulated by both fatty acid and acyl-CoA binding proteins (35,36). As an example of insufficient regulation, it was reported that the concentration of long-chain fatty acyl-CoA esters in the muscle of obese Zucker rats increased three times more than the concentration of acyl-CoA binding protein when compared with lean rats (37). This finding shows that under some conditions, the concentration of the free cytosolic long-chain fatty acyl-CoA esters can also increase in vivo.

Bakker et al. (6,7) hypothesized that the inhibition of mitochondrial adenine nucleotide translocator by the increased concentration of cytosolic long-chain fatty acyl-CoA esters might be among the key mechanisms underlying β-cell dysfunction. In this study we have investigated the effect of 5 μmol/l palmitoyl-CoA on oxidative phosphorylation in isolated rat liver mitochondria. Literature reports suggest that palmitoyl-CoA acts on adenine nucleotide translocator (9), but its effect on the other components of mitochondrial oxidative phosphorylation was not determined previously. To determine the sites of the direct action of palmitoyl-CoA in oxidative phosphorylation, we applied modular kinetic (or top-down elasticity) analysis. This type of analysis was previously successfully applied to determine the sites of action of different external effectors in oxidative phosphorylation (19,38,39). We divided mitochondrial oxidative phosphorylation in two different ways, as illustrated in Fig. 1. Under the experimental conditions used, 5 μmol/l palmitoyl-CoA exclusively inhibited adenine nucleotide translocator, and this inhibition led to an increase in Δψ and ATP concentration in the mitochondrial matrix. The addition of 5 μmol/l palmitoyl-CoA had no direct effect on the other components of oxidative phosphorylation or on the proton permeability of the mitochondrial membrane. The latter finding also shows that there were no detergent-type interactions of palmitoyl-CoA with the membranes. Although we found a single direct effect of palmitoyl-CoA, there were many indirect effects that depended on the way mitochondrial oxidative phosphorylation was managed:

- When the substrates for both respiration and phosphorylation were in excess, 5 μmol/l palmitoyl-CoA had a strong effect on both the phosphorylation rate (which decreased by 38%) and Δψ (which increased by 15 mV). Indeed, recently it was shown that the insulin-resistant offspring of patients with type 2 diabetes had a 30% reduced rate of mitochondrial oxidative phosphorylation when compared with control subjects (40). The effects on the external and matrix fraction of ATP were opposite: the external fraction of ATP decreased by 39%, whereas the fraction of matrix ATP increased by 46%. The conditions of this particular experiment could reflect the situation that occurs during type 2 diabetes in cell types that have insulin-independent glucose uptake (such us endothelial and β-cells). These tissues have excess redox equivalent supply caused primarily by increased levels of fatty acids and secondarily by hyperglycemia. Similar changes in cytosolic and matrix ATP levels in response to increased long-chain fatty acyl-CoA esters were observed by Soboll et al. (41) in intact rat liver cells. A prolonged decrease in the cytosolic fraction of ATP (as expected from our in vitro experiments) might lead to the opening of ATP-sensitive K^+ channels, which play an important role in the insulin release in β-cells (42). This effect would be amplified by the reported direct stimulation of channel opening by long-chain fatty acyl-CoA esters (43–46).
- In the situation where mitochondrial oxidative phosphorylation is managed by a constant supply of redox equivalents, the initial decrease of respiration caused by palmitoyl-CoA should be overcome by an increased redox potential returning the reducing equivalent flux to the initial value. In this situation palmitoyl-CoA caused a much higher increase in ATP concentration in the matrix and a much higher increase in Δψ than when all substrates were in excess. Importantly, now extramitochondrial ATP was not affected by palmitoyl-CoA (Table

1, *row B* minus *row C*). When the extramitochondrial ATP-consumption flux was maintained constant, $\Delta\psi$ and the fractions of matrix ATP were not affected at all by 5 μmol/l palmitoyl-CoA, but the extramitochondrial ATP was affected dramatically (*row B* minus *row D*).

Our experiments showed that the extramitochondrial AMP concentration increased in a palmitoyl-CoA concentration–dependent manner. Increased AMP concentration might lead to extra adenosine formation (affecting glucose uptake) (11–13) as well as activation of ATP synthesis mediated by AMP-activated protein kinase (47,48). The latter, however, is hindered by inhibition of adenine nucleotide translocator by long-chain fatty acyl-CoA esters.

Modular kinetic analysis as applied by us may be useful more generally for (medical) systems biology. The method enables one to define the site of the molecular action of agents that have widespread effects on many functions, such as palmitoyl-CoA. It gives insight in how a single agent working on a single molecular target has a multitude of indirect effects, the relative severity of which depends on the regulatory condition. Indeed, notwithstanding its multifarious effects on functional properties such as $\Delta\psi$, matrix ATP, cytosolic ATP, and AMP, the action of palmitoyl-CoA was localized unequivocally to the adenine nucleotide translocator (Figs. 4*A* and 5). Obesity and type 2 diabetes are characterized by different effects that vary depending on the tissues and individuals. This might suggest that many molecular factors and targets are involved. This article shows that a single primary molecular mechanism might still account for much of the substantial variety of the effects of long-chain fatty acyl-CoA esters in different tissues. In addition, the data presented give direct information about the relative effects on this flux of the two factors expected to determine the flux through adenine nucleotide translocator (fraction of matrix ATP and $\Delta\psi$).

ACKNOWLEDGMENTS

This research was funded by the Dutch Diabetes Foundation (grant 1999.007).

The authors are grateful to G. Wardeh for rat livers.

REFERENCES

1. Schneider SH, Khachadurian AK, Amorosa LF, Clemow L, Ruderman NB: Ten-year experience with an exercise-based outpatient life-style modification program in the treatment of diabetes mellitus. *Diabetes Care* 15:1800–1810, 1992
2. Ruderman NB, Chisholm D, Pi-Sunyer X, Schneider SH: The metabolically obese, normal-weight individual revisited. *Diabetes* 47:699–713, 1998
3. Unger RH: Lipotoxic diseases. *Annu Rev Med* 53:319–336, 2002
4. Reaven GM, Hollenbeck C, Jeng CY, Wu MS, Chen YD: Measurement of plasma glucose, free fatty acid, lactate, and insulin for 24 h in patients with NIDDM. *Diabetes* 37:1020–1024, 1988
5. Walker KZ, O'Dea K, Johnson L, Sinclair AJ, Piers LS, Nicholson GC, Muir JG: Body fat distribution and non-insulin-dependent diabetes: comparison of a fiber rich, high carbohydrate, low-fat (23%) diet and a 35% fat diet high in monounsaturated fat. *Am J Clin Nutr* 63:254–260, 1996
6. Bakker SJL, IJzerman RG, Teerlink T, Westerhoff HV, Gans ROB, Heine RJ: Cytosolic triglycerides and oxidative stress in central obesity: the missing link between excessive atherosclerosis, endothelial dysfunction, and β-cell failure? *Atherosclerosis* 148:17–21, 2000
7. Bakker SJL, Gans ROB, ter Maaten JC, Teerlink T, Westerhoff HV, Heine RJ: The potential role of adenosine in the pathophysiology of the insulin resistance syndrome. *Atherosclerosis* 155:283–290, 2000
8. Klingenberg M: The adenine-nucleotide exchange in submitochondrial (sonic) particles. *Eur J Biochem* 76:553–565, 1977
9. Chua BH, Shrago E: Reversible inhibition of adenine nucleotide translocation by long chain acyl-CoA esters in bovine heart mitochondria and inverted submitochondrial particles. *J Biol Chem* 252:6711–6714, 1977
10. Burdon RH: Superoxide and hydrogen peroxide in relation to mammalian cell proliferation. *Free Radic Biol Med* 18:775–794, 1995
11. Espinal J, Challiss JRA, Newshome EA: Effect of adenosine deaminase and an adenosine analogue on insulin sensitivity in soleus muscle of the rat. *FEBS Lett* 158:103–106, 1983
12. Han DH, Hansen PA, Nolte LA, Holloszy JO: Removal of adenosine decreases the responsiveness of muscle glucose transport to insulin and contractions. *Diabetes* 47:1671–1675, 1998
13. Challiss JRA, Budohoski L, McManus B, Newshome EA: Effects of an adenosine-receptor antagonist on insulin-resistance in soleus muscle from obese Zucker rats. *Biochem J* 221:915–917, 1984
14. Brand MD: Top-down elasticity analysis and its application to energy metabolism in isolated mitochondria and intact cells. *Mol Cell Biochem* 184:13–20, 1998
15. Dodge JT, Phillips GB: Composition of phospholipids and of phospholipid fatty acids and aldehydes in human red cell. *J Lipid Res* 8:667–675, 1967
16. Mildaziene V, Nauciene Z, Baniene R, Grigiene J: Multiple effects of 2,2,5,5-tetrachlorbiphenyl on oxidative phosphorylation in rat liver mitochondria. *Toxicol Sci* 65:220–227, 2002
17. Bradford MM: A rapid and sensitive method for the quantification of microgram quantities of protein utilizing the principle of protein-dye binding. *Anal Biochem* 72:248–254, 1976
18. Borutaite V, Mildaziene V, Brown GC, Brand MD: Control and kinetic analysis of ischemia-damaged heart mitochondria: which parts of the oxidative phosphorylation system are affected by ischemia? *Biochim Biophys Acta* 1272:154–158, 1995
19. Marcinkeviciute A, Mildaziene V, Crumm S, Demin O, Hoek JB, Kholodenko B: Kinetics and control of oxidative phosphorylation in rat liver mitochondria after chronic ethanol feeding. *Biochem J* 349:519–526, 2000
20. Jensen PR, Westerhoff HV, Michelsen O: Excess capacity of H^+-ATPase and inverse respiratory control in *Escherichia coli*. *EMBO J* 12:1277–1282, 1993
21. Jaworek D, Gruber W, Bergmeyer HU: Adenosine-5′-diphosphat und adenosin-5′-monophosphat. In *Methoden der Enzymatishen Analyse*. Vol. 2, 3rd ed. Bergmeyer HU, Ed. Weinheim, Germany, Verlag Chemie, 1974, p. 2178–2181
22. Schatz G: Oxidative phosphorylation. In *Methods in Enzymology*. Vol. 10. Estabrook RW, Pullman ME, Eds. New York, Academic Press, 1967, p. 26–27
23. Hohorst HJ: D-glucose-6-phosphat und D-fructose-6-phosphat. In *Methoden der Enzymatishen Analyse*. Vol. 2, 3rd ed. Bergmeyer HU, Ed. Weinheim, Germany, Verlag Chemie, 1974, p. 1200–1204
24. Hinkle PC: Measurement of ADP/O ratios. In *Bioenergetics: A Practical Approach*. Brown GC, Cooper CE, Eds. Oxford, U.K., IRL Press, 1995, p. 5–6
25. Hafner RP, Brown GC, Brand MD: Analysis of the control of respiration rate, phosphorylation rate, proton leak rate and protonmotive force in isolated mitochondria using the 'top-down' approach of metabolic control theory. *Eur J Biochem* 188:313–319, 1990
26. Kunst A, Draeger B, Ziegenhorn J: UV-methods with hexokinase and glucose-6-phosphate dehydrogenase. In *Methods of Enzymatic Analysis*. Vol. 6, 3rd ed. Bergmeyer HU, Ed. Weinheim, Germany, Verlag Chemie, 1984, p. 163–172
27. Wanders RJA, Van Woerkom GM, Nooteboom RF, Meijer AJ, Tager JM: Relationship between the rate of citrulline synthesis and bulk changes in the intramitochondrial ATP/ADP ratio in rat-liver mitochondria. *Eur J Biochem* 113:295–302, 1981
28. Brand MD, Chien LF, Ainscow EK, Rolfe DFS, Porter RK: The causes and functions of mitochondrial proton leak. *Biochim Biophys Acta* 1187:132–139, 1994
29. Dufour S, Rousse N, Cnioni P, Diolez P: Top-down control analysis of temperature effect on oxidative phosphorylation. *Biochem J* 314:743–751, 1996
30. Crielaard W, Cotton NPJ, Jackson JB, Heilingwerf KJ, Konings WN: The transmembrane electrical potential in intact bacteria: simultaneous measurements of caratenoid absorbance changes and lipophilic cation distribution in intact cells of *Rhodobacter sphaeroides*. *Biochim Biophys Acta* 932:17–25, 1988
31. Brdiczka D, Pette D, Brunner G, Miller F: [Compartmental dispersion of enzymes in rat liver mitochondria]. *Eur J Biochem* 5:294–304, 1968

32. Faergeman NJ, Knudsen J: Role of long-chain fatty acyl-CoA esters in the regulation of metabolism and cell signaling. *Biochem J* 323:1–12, 1997
33. Sterchele PF, Vanden Heuvel JP, Davis II JW, Shrago E, Knudsen J, Peterson RE: Induction of hepatic acyl-CoA-binding protein and liver fatty acid-binding protein by perfluorodecanoic acid in rats: lack of correlation with hepatic long-chain acyl-CoA levels. *Biochem Pharmacol* 48:955–966, 1994
34. Prentki M, Vischer S, Glennon MC, Regazzi R, Deeney JT, Corkey BE: Malonyl-CoA and long chain acyl-CoA esters as metabolic coupling factors in nutrient-induced insulin secretion. *J Biol Chem* 267:5802–5810, 1992
35. Mishkin S, Turcotte R: The binding of long chain fatty acid CoA to Z, a cytoplasmic protein present in liver and other tissues of the rat. *Biochem Biophys Res Commun* 57:918–926, 1974
36. Mogensen IB, Schulenberg H, Hansen HO, Spener F, Knudsen J: A novel acyl-CoA-binding protein from bovine liver: effect on fatty acid synthesis. *Biochem J* 241:189–192, 1987
37. Franch J, Knudsen J, Ellis BA, Pedersen PK, Cooney GJ, Jensen J: Acyl-CoA binding protein expression is fiber type-specific and elevated in muscles from obese insulin-resistant Zucker rat. *Diabetes* 51:449–454, 2002
38. Kesseler A, Brand MD: Localisation of the sites of action of cadmium on oxidative phosphorylation in potato tuber mitochondria using top-down elasticity analysis. *Eur J Biochem* 225:897–906, 1994
39. Krab K, Wagner MJ, Wagner AM, Moler IM: Identification of the site where the electron transfer chain of plant mitochondria is stimulated by electrostatic charge screening. *Eur J Biochem* 267:869–876, 2000
40. Petersen KF, Dufour S, Befroy D, Garcia R, Shulman GI: Impaired mitochondrial activity in the insulin-resistant offspring of patients with type 2 diabetes. *N Engl J Med* 350:664–671, 2004
41. Soboll S, Seitz HJ, Sies H, Ziegler B, Scholz R: Effect of long-chain fatty acyl-CoA on mitochondrial and cytosolic ATP/ADP ratios in the intact liver cell. *Biochem J* 220:371–376, 1984
42. Rustenbeck I: Desensitization of insulin secretion. *Biochem Pharmacol* 63:1921–1935, 2002
43. Larsson O, Deeney JT, Bränström R, Berggren PO, Corkey BE: Activation of the ATP-sensitive K^+ channel by long chain acyl-CoA: a role in modulation of pancreatic beta-cell glucose sensitivity. *J Biol Chem* 271: 10623–10626, 1996
44. Bränström R, Corkey BE, Berggren PO, Larsson O: Evidence for a unique long chain acyl-CoA ester binding site on the ATP-regulated potassium channel in mouse pancreatic beta cells. *J Biol Chem* 272:17390–17394, 1997
45. Gribble FM, Proks P, Corkey BE, Ashcroft FM: Mechanism of cloned ATP-sensitive potassium channel activation by oleoyl-CoA. *J Biol Chem* 273:26383–26387, 1998
46. Bränström R, Leibiger IB, Leibiger B, Corkey BE, Berggren PO, Larsson O: Long chain coenzyme A esters activate the pore-forming subunit (Kir6. 2) of the ATP-regulated potassium channel. *J Biol Chem* 273:31395–31400, 1998
47. Rutter GA, Da Silva Xavier G, Leclerc I: Roles of 5′-AMP-activated protein kinase (AMPK) in mammalian glucose homeostasis. *Biochem J* 375:1–16, 2003
48. Carling D: The AMP-activated protein kinase cascade—a unifying system for energy control. *Trends Biochem Sci* 29:18–24, 2004